Appendix

Table. A1. Summary of previous studies on long-term trends of near-surface wind speed over the Tibetan Plateau using 10-m anemometer observations where more than 10 stations were used (The current study is included for completeness, and they are ordered chronologically by year and then alphabetically).

No.	Reference	No. of stations	Period	Homogenized	Trend (m s^{-1} per decade)	Main finding
1	Lin et al., 2013	125	1960–2009	No	**–0.06**	Overall decrease of wind speed in annual and all seasons
2	Yao and Li, 2016	73	1971–2012	No	–0.25*	Spring wind speed consistently declined,with a smaller magnitude after 1998
3	Guo et al., 2017	139	1970–2012	No	–0.201*	Annual wind speed decreased in the whole area, with the decreasing rate amplified with increasing elevation
4	Yang et al., 2020	11	1980–2015	No	–0.181*	Wind speed has generally decreased on both annual and seasonal bases since 1980
5	This study	104	1961–2020	Yes	**–0.091**	Wind speed significantly declined, with a distinct increase during 1961– 1970, a significant decrease during 1970–2002, and a consistent increase since 2002

Note: Statistically significant trends at $p < 0.05$ are bolded, * indicates that the significance level was not shown in the reference.

Table. A2. Description of atmospheric circulation indices representing Asian monsoon and westerlies modes.

Index	Definition	Reference
East Asian summer monsoon index (EASMI)	Defined as an area-averaged seasonally (June–August) dynamical normalized seasonality (DNS) at 850 hPa within the East Asian monsoon domain (10°–40°N, 110°–140°E)	Li and Zeng, 2002
Indian summer monsoon index (ISMI)	Defined using the difference of the 850-hPa zonal winds between a southern region of 5°–15°N, 40°–80°E and a northern region of 20°–30°N, 70°–90°E	Wang et al., 2001
East Asian winter monsoon index (EAWMI)	Defined as the mean geopotential height at 500 hPa in the area of25°–45°N, 110°–145°E	Wang and He, 2012
Westerly Index (WI)	Defined as the average zonal index in five zones of 30 longitude intervals within the 45°–65°N, 0°–150°E regions at 500 hPa	Vicente-Serrano et al., 2016
Tibetan Plateau index (TPI)	Defined as the cumulative value of the difference between the geopotential height of the grid and 5000 geopotential meters multiplied by the area of the grid, within 30°–40°N, 75°–105°E regions at 500 hPa	You et al., 2014

Table. A3. Frequency (%) of the 104 TP stations that exhibited positive and negative trends of near-surface wind speed at annual and seasonal time scales from 1961–2020 and three subperiods (*i.e.*, 1961–1970, 1970–2002, 2002–2020).

Period	Season	Negative trend	Significantly negative ($p < 0.05$)	Positive trend	Significantly positive ($p < 0.05$)
1961–2020	Annual	100.0	87.5	0.0	0.0
	Winter	93.3	73.2	6.7	0.0
	Spring	100.0	91.3	0.0	0.0
	Summer	95.2	72.7	4.8	20.0
	Autumn	96.2	78.0	3.8	0.0
1961–1970	Annual	25.0	11.5	75.0	26.9
	Winter	20.2	4.8	79.8	22.9
	Spring	31.7	3.0	68.3	14.1
	Summer	26.0	7.4	74.0	24.7
	Autumn	25.0	15.4	75.0	15.4
1970–2002	Annual	100.0	100.0	0.0	0.0
	Winter	100.0	97.1	0.0	0.0
	Spring	100.0	98.1	0.0	0.0
	Summer	100.0	97.1	0.0	0.0
	Autumn	100.0	99.0	0.0	0.0
2002–2020	Annual	47.1	16.3	52.9	41.8
	Winter	35.6	10.8	64.4	26.9
	Spring	65.4	30.9	34.6	22.2
	Summer	30.8	12.5	69.2	41.7
	Autumn	26.9	14.3	73.1	42.1

Table. A4. Correlations of annual and seasonal wind speed simulated by westerly and Asian monsoon modes with observed wind speed for the three sub-periods in the Tibetan Plateau.

Season	1961–1970	1970–2002	2002–2020
Annual	**0.72**	**0.71**	**0.65**
Winter	**0.66**	**0.62**	**0.53**
Spring	**0.82**	**0.59**	0.36
Summer	**0.75**	**0.75**	**0.54**
Autumn	**0.61**	**0.83**	**0.69**

Note: Statistically significant trends ($p < 0.05$) are bolded.

Table. A5. Trends in annual and seasonal near-surface wind speed (m s^{-1} per decade) for the Tibetan Plateau calculated by raw wind speed data.

Season	1961–2020	1961–1970	1970–2002	2002–2020
Annual	**−0.09**	**0.38**	**−0.25**	**0.08**
Winter	**−0.07**	**0.68**	**−0.26**	0.07
spring	**−0.13**	0.36	**−0.28**	−0.01
summer	**−0.07**	**0.41**	**−0.24**	**0.10**
Autumn	**−0.06**	**0.43**	**−0.21**	**0.14**

Note: Statistically significant values ($p < 0.05$) are bolded.

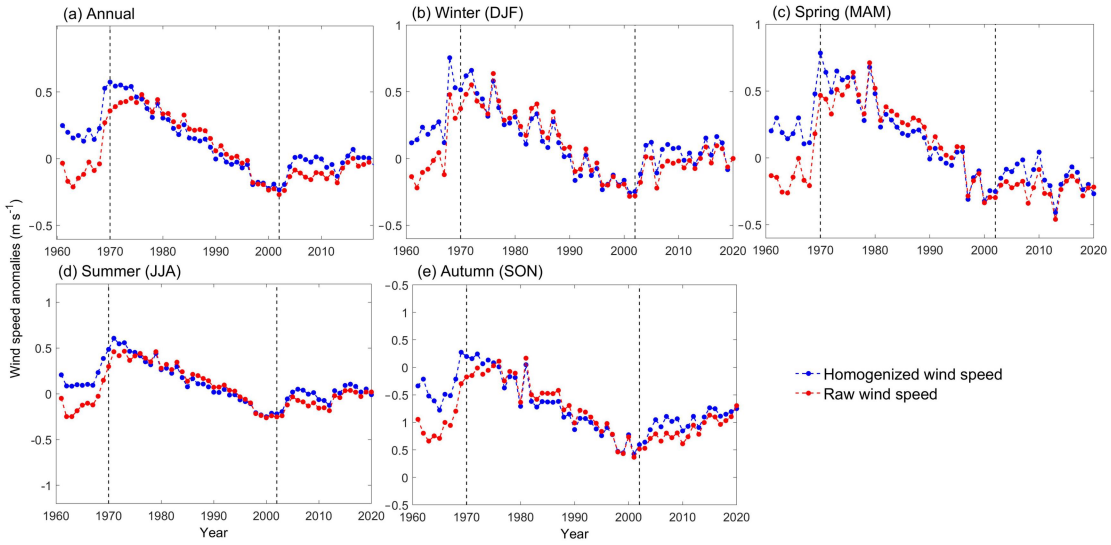

Fig. A1. Annual and seasonal mean near-surface wind speed anomalies relative to 1981–2010 based on raw wind speed and homogenized wind speed over the Tibet Plateau for 1961–2020.

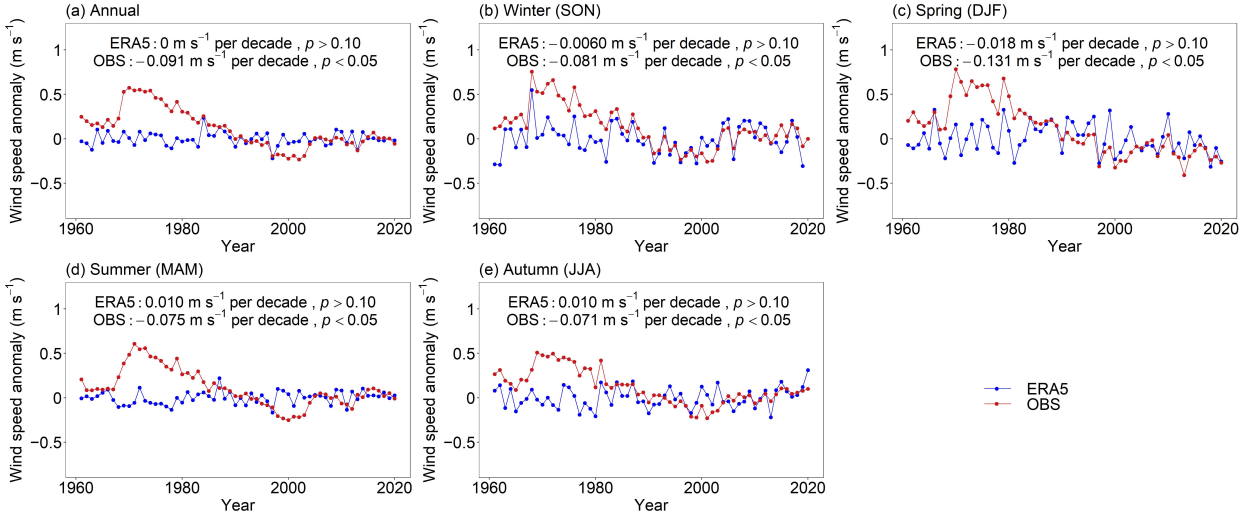

Fig. A2. Annual and seasonal mean near-surface wind speed anomalies based on observations (OBS) and ERA5 over the Tibet Plateau for 1961–2020 (relative to the 1981–2010 mean).

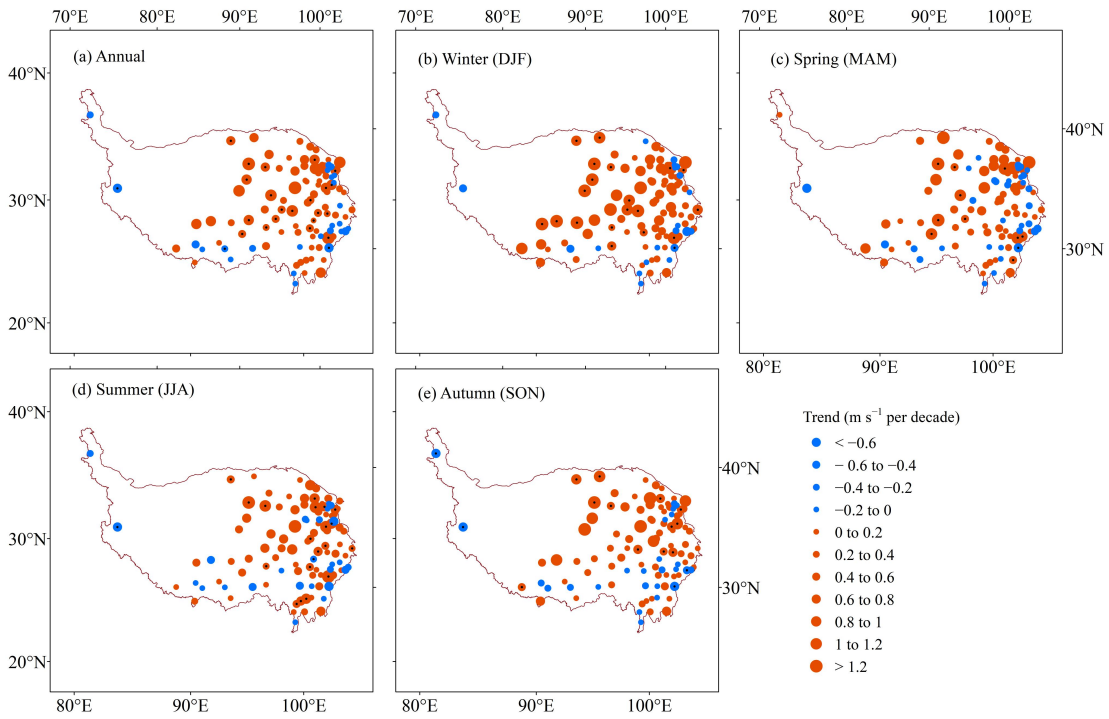

Fig. A3. Spatial distribution of the sign and magnitude of annual and seasonal observed near-surface wind speed trends over the Tibet Plateau for 1961–1970 (The black dot in the circle represents a statistically significant trend at $p < 0.05$).

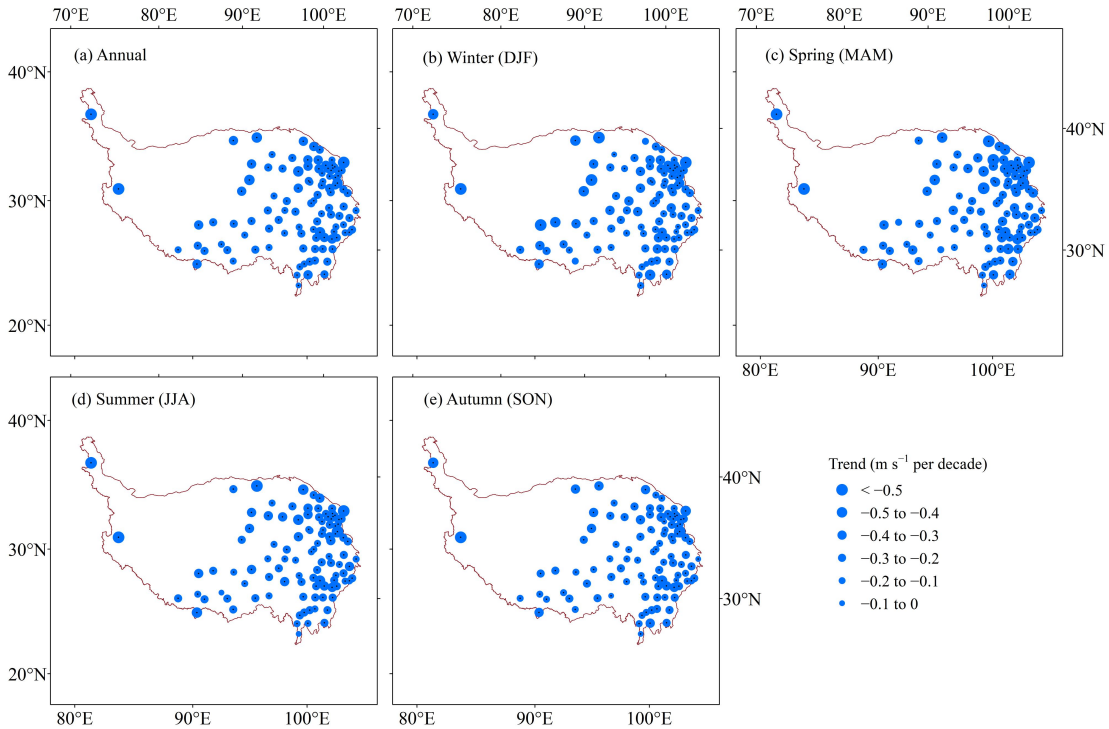

Fig. A4. Spatial distribution of the sign and magnitude of annual and seasonal observed near-surface wind speed trends over Tibet Plateau for 1970–2002 (The black dot in the circle represents a statistically significant trend at $p < 0.05$).

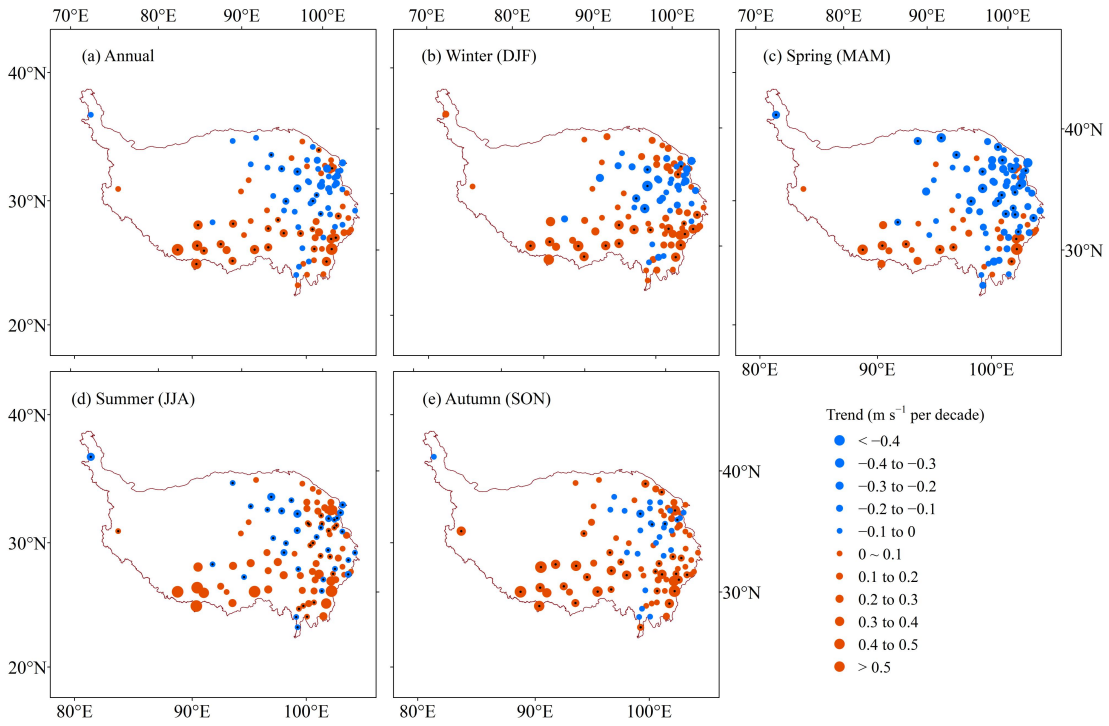

Fig. A5. Spatial distribution of the sign and magnitude of annual and seasonal observed near-surface wind speed trends over Tibet Plateau for 2002–2020 (The black dot in the circle represents a statistically significant trend at $p < 0.05$).

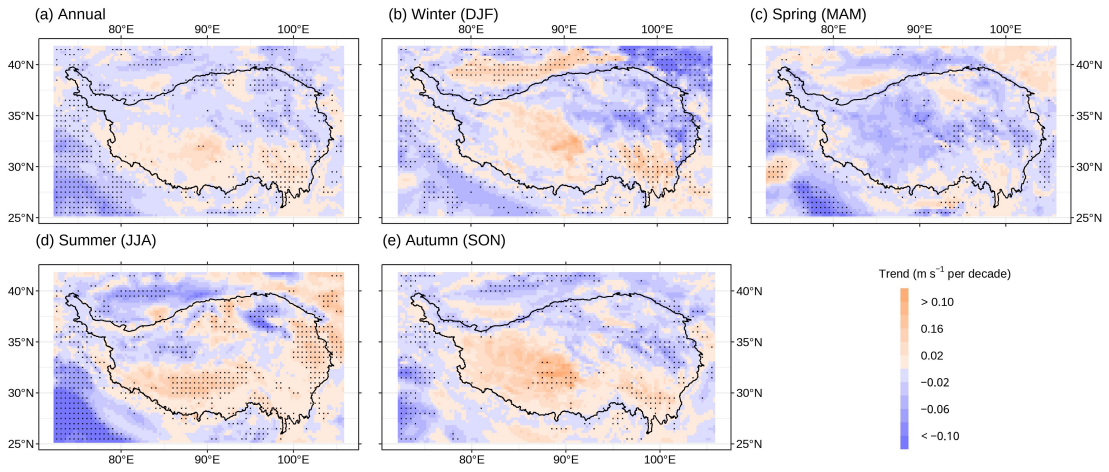

Fig. A6. Spatial distribution of the sign and magnitude of annual and seasonal near-surface wind speed trends from ERA5 over the Tibet Plateau for 1961–2020 (The black dot represents a statistically significant trend at $p < 0.05$).

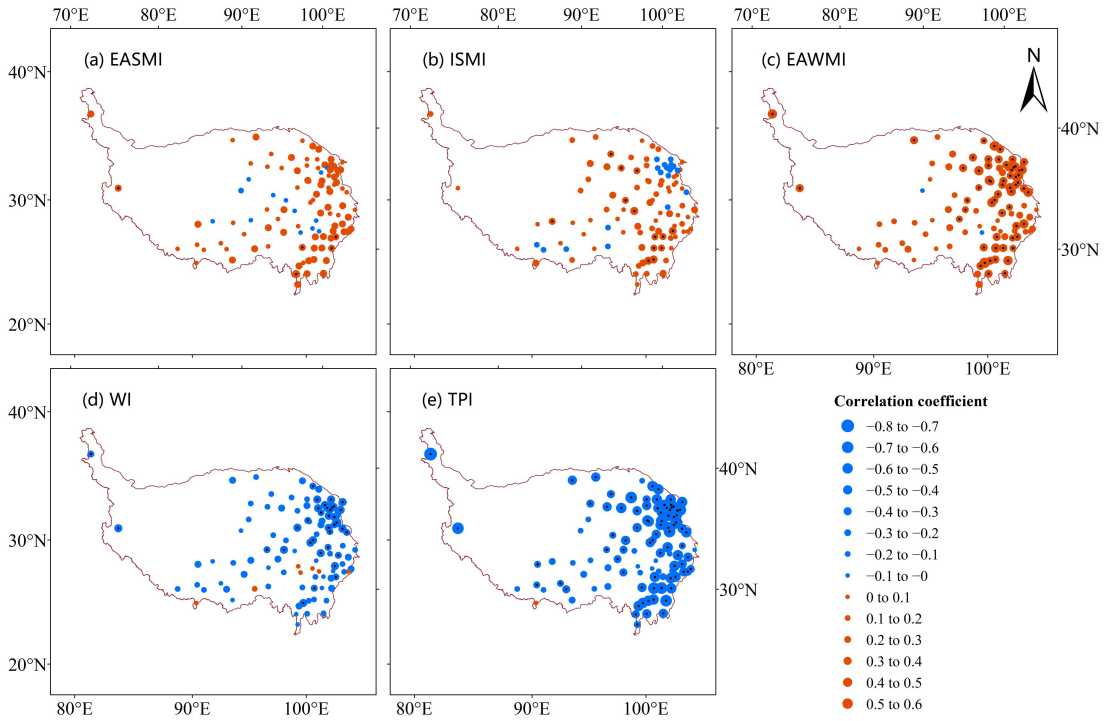

Fig. A7. Spatial distribution of the sign, magnitude, and statistical significance of Pearson's correlation coefficients between observed annual wind speed and the EASMI, ISMI, EAWMI, WI and TPI across the TP (A small black dot in a circle indicates a significant correlation at $p < 0.05$).

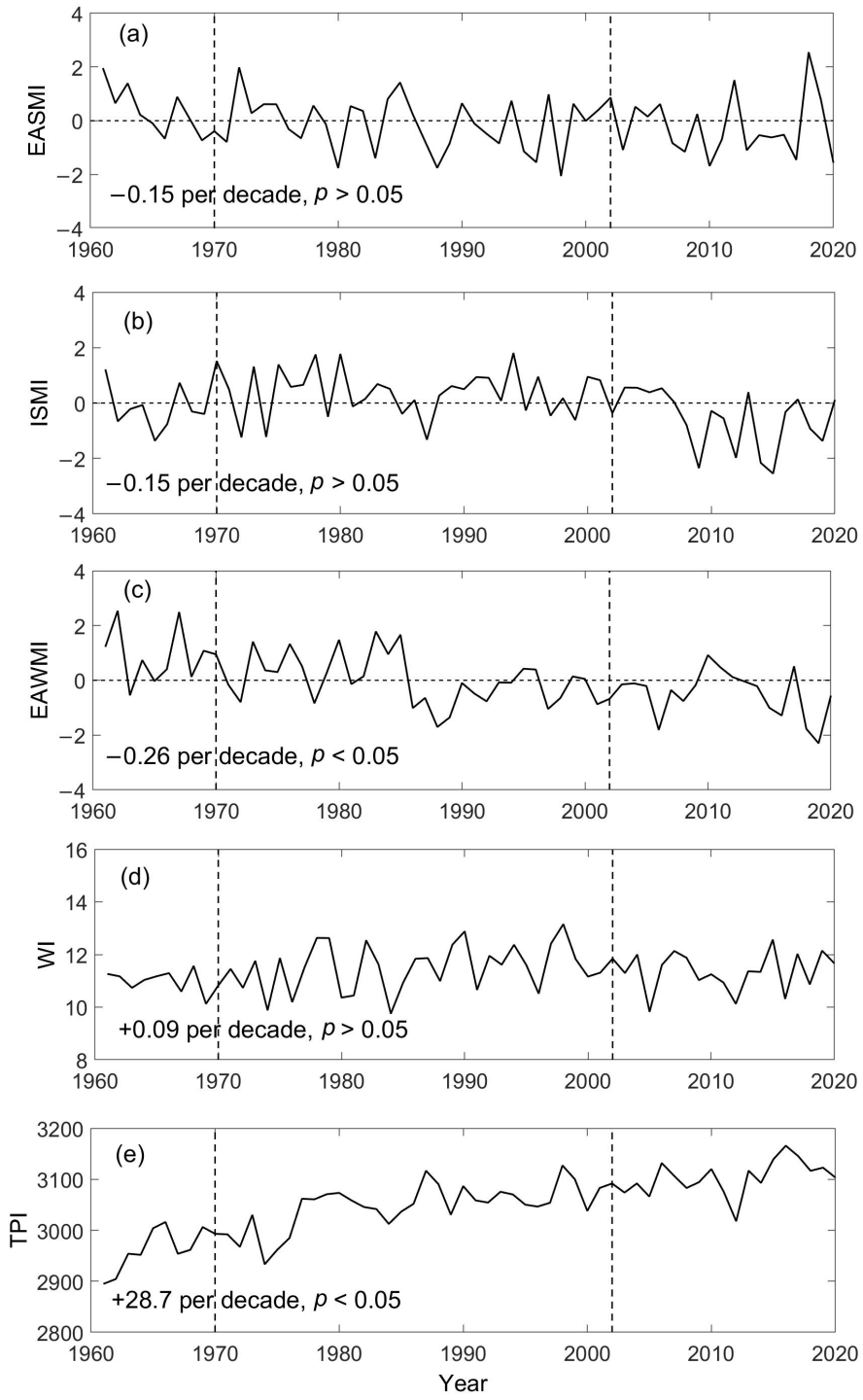

Fig. A8. Variability of westerly and Asian monsoon modes from 1961–2020 (The two dashed vertical lines (years 1970 and 2002) indicate the division of the three sub-periods of near-surface wind speed changes).

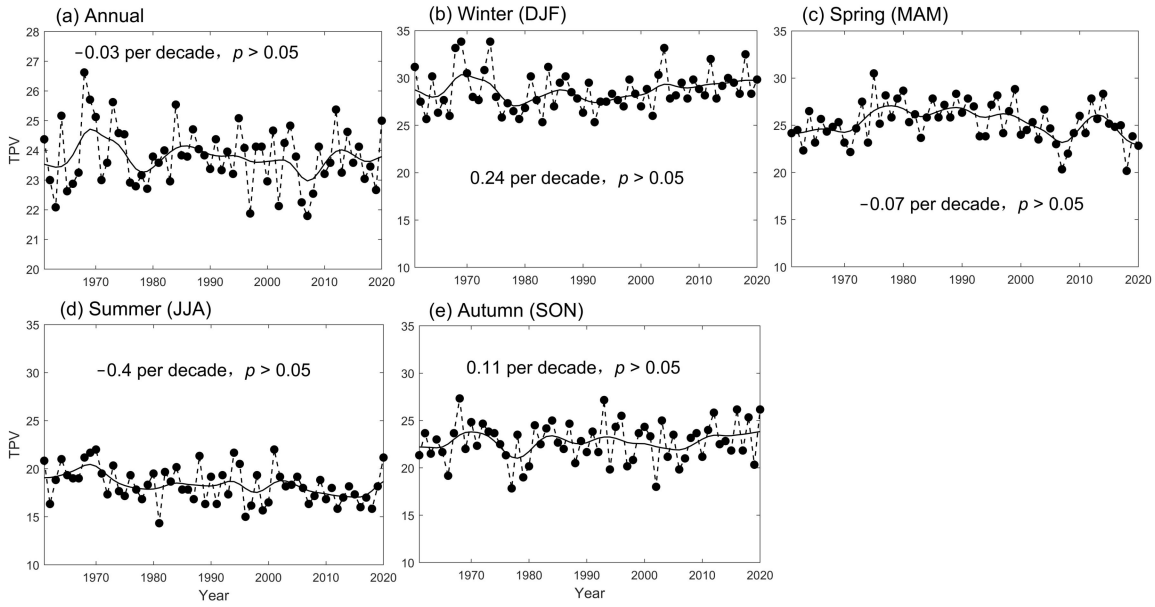

Fig. A9. Annual and seasonal TPV (Tibetan Plateau vortex) variability and trends (The 11-year Gaussian low-pass filter is illustrated as the black solid line).

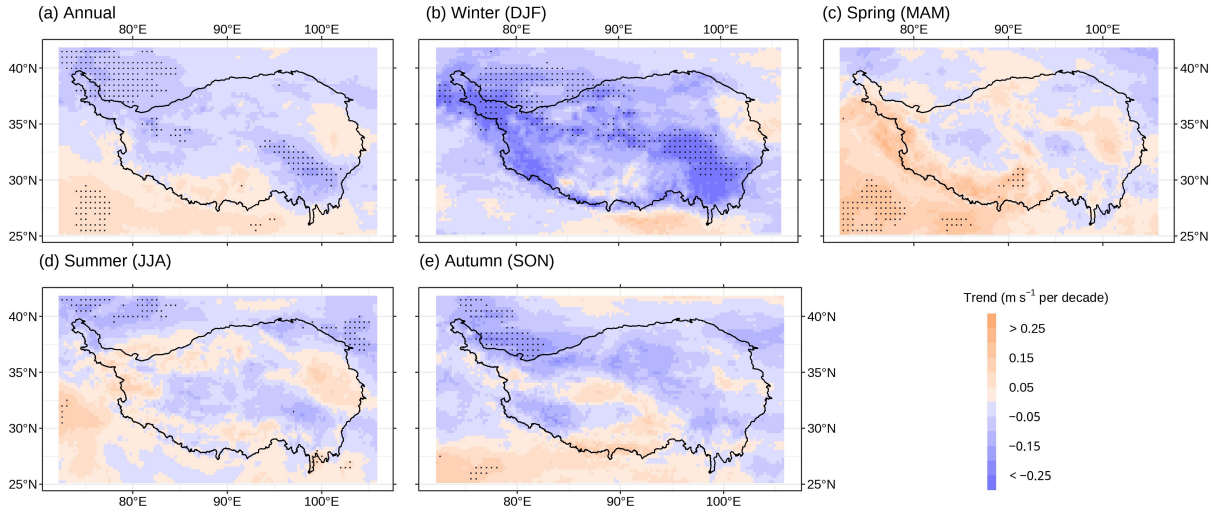

Fig. A10. Spatial distribution of the annual and seasonal vertical wind shear trends between 450 hPa and 500 hPa across the Tibet Plateau and surrounds for 1970–2002 (A small black star represents a grid cell ($0.25^{o} \times 0.25^{o}$) with a significant trend at $p < 0.05$).

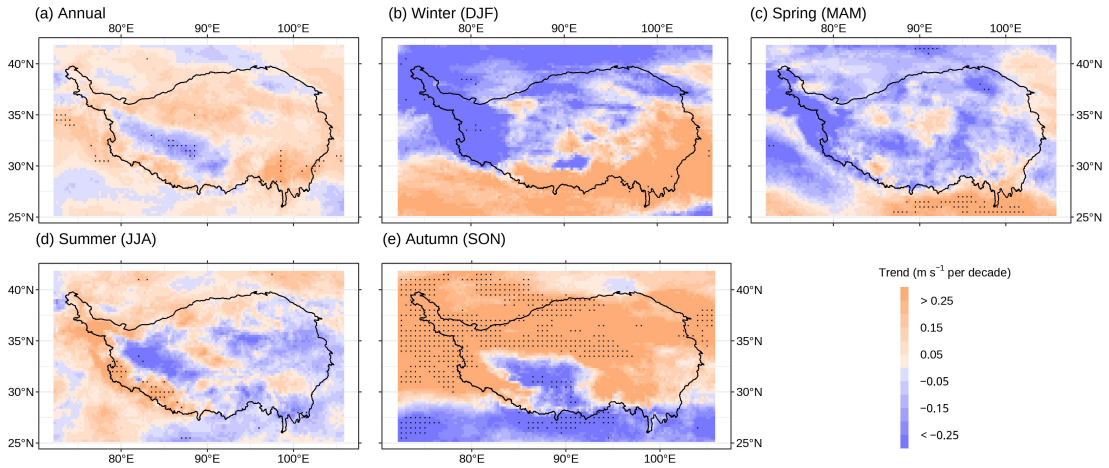

Fig. A11. Spatial distribution of the annual and seasonal vertical wind shear trends between 450 hPa and 500 hPa across the Tibet Plateau and surrounds for 2002–2020 (A small black star represents a grid cell ($0.25^{o} \times 0.25^{o}$) with a significant trend at $p < 0.05$).

References

Guo, X., Wang, L., Tian, L., et al., 2017. Elevation-dependent reductions in wind speed over and around the Tibetan Plateau. Int. J. Climatol. 37, 1117–1126. https://doi.org/10.1002/joc.4727

Li, J., Zeng, Q., 2002. A unified monsoon index. Geophys. Res. Lett. 29, 1–4. https://doi.org/10.1029/2001GL013874.

Lin, C., Yang, K., Qin, J., et al., 2013. Observed coherent trends of surface and upper-air wind speed over China since 1960. J. Clim. 26, 2891–2903. https://doi.org/10.1175/JCLI-D-12-00093.1.

Vicente-Serrano, S.M., García-Herrera, R., Barriopedro, D.,et al., 2016. The Westerly Index as complementary indicator of the North Atlantic oscillation in explaining drought variability across Europe. Clim. Dyn. 47, 845–863. https://doi.org/10.1007/s00382-015-2875-8.

Wang, B., Wu, R., Lau, K.M., 2001. Interannual variability of the asian summer monsoon: contrasts between the Indian and the Western North Pacific–East Asian monsoons. J. Clim. 14, 4073–4090. https://doi.org/10.1175/1520-0442(2001)014<4073:IVOTAS>2.0.CO;2.

Wang, H., He, S., 2012. Weakening relationship between East Asian winter monsoon and ENSO after mid-1970s. Chinese Sci. Bull. 57, 3535–3540. https://doi.org/10.1007/s11434-012-5285-x

Yang, J., Xia, D., Wang, S., et al., 2020. Near-surface wind environment in the Yarlung Zangbo River basin, southern Tibetan Plateau. J. Arid Land 12, 917–936. https://doi.org/10.1007/s40333-020-0104-8.

Yao, H., Li, D., 2016. The interannual variation of wind speed in the Tibetan Plateau in spring and its response to global warming during 1971–2012. Acta Meteorol. Sin. 74, 60–75.

You, Q., Fraedrich, K., Min, J., et al., 2014. Observed surface wind speed in the Tibetan Plateau since 1980 and its physical causes. Int. J. Climatol. 34, 1873–1882. https://doi.org/10.1002/joc.3807.